Imaging Human Structures

Byung-Tae Kim[1], Yong Choi[1], Joung Hwan Mun[2], Dae-Weon Lee[2],
Sung Min Kim[3]

[1]Department of Nuclear Medicine, Samsung Medical Center,
Sungkyunkwan University School of Medicine
[2]Department of Bio-Mechatronic Engineering, Sungkyunkwan University
[3]Department of Biomedical Engineering, Konkuk University
*Center for Imaging Human Structures

Abstract: The Center for Imaging Human Structures (CIH) was established in December 2002 to develop new diagnostic imaging techniques and to make them available to the greater community of biomedical and clinical researchers at Sungkyunkwan University.
CIH has been involved in 5 specific activities to provide solutions for early diagnosis and improved treatment of human diseases. The five area goals include: 1) development of a digital mammography system with computer aided diagnosis (CAD); 2) development of digital radiological imaging techniques; 3) development of unified medical solutions using 3D image fusion; 4) development of multi-purpose digital endoscopy; and, 5) evaluation of new imaging systems for clinical application

DIGITAL MANNOGRAPHY SYSTEM WITH COMPUTER AIDED DIAGNOSIS(CAD)

The aim of this project is the development of a full-field digital mammography system with high resolution digital X-ray and a computer aided diagnosis (CAD) system which detects and displays breast cancer.

We have developed software for the automatic detection of solid tumor cancers in digital mammography and we have designed software that provides robust information against the noise and background brightness of digital mammography. Preliminary experimental results support the hypothesis that the mass detection performance of this method is a possible solution for identifying solid tumor cancers.

Corresponding Author : Yong Choi
Department of Nuclear Medicine, Samsung Medical Center, Sungkyunkwan University School of Medicine, 50 Ilwon-dong, Kangnam-ku,Seoul, 135-710 Korea
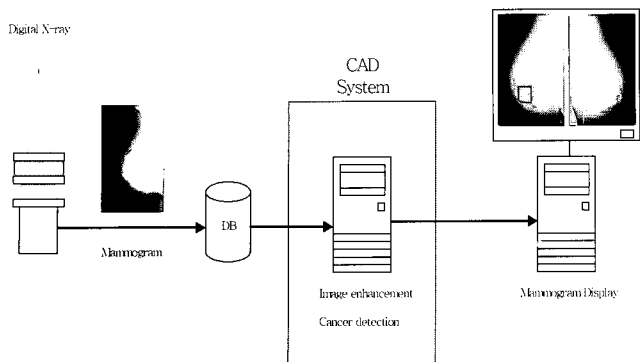Tel. 02-3410-2624   Fax. 02-3410-2639
E-mail. ychoi@skku.edu

Microcalcification detection is a major part of the diagnosis of early stages of breast cancer [1]. In this project, we propose a microcalcification detection system consisting of a pre-processing mammogram module and a microcalcification detection module. In the pre-processing, contrast enhancement and background segmentation are performed. The microcalcification detection module contains a multi-stage Artificial Neural Network (ANN).

The entire proposed system is shown in Fig. 1, which illustrates digital mammography. The digital image is stored in the Data Base (DB) and some diagnostic results are recorded and displayed in the screen. The proposed system detects microcalcification with CAD. To detect microcalcification, breast segmentation, contrast enhancement and multistage ANN are used. Results of microcalcification detection are stored in DICOM format and displayed by a mammogram viewer within the system. These results help detect microcalcification, and provide background information for a subsequent biopsy to the physician.

The overall scheme of proposed microcalcification detection is shown in Fig. 2.

Microcalcification detection is composed of image pre-processing, image enhancement and detection that uses multistage ANN.

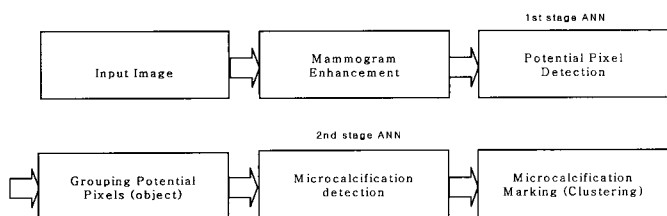**Fig. 1.** Proposed CAD system of digital mammography

Fig. 2. Proposed microcalcification detection

Mammogram Enhancement

In mammograms, high attenuation properties and the small size of microcalcifications are major reasons for the poor visualization of small lesions. To improve the visibility of breast cancers, image enhancement methods have been performed [2-5]. The homomorphic filter function decreases the energy of low frequencies while increasing those of high frequencies in the image. With any given mammogram, the homomorphic filter provides contrast stretching for the lower gray level by compressing the dynamic range of it. Based on these properties, we implemented homomorphic filtering in the wavelet domain with de-noising of the given image [3]. Fig. 3 (a) shows an original image and a homomorphic enhanced image. In Fig. 3 (b), the pattern of microcalcifications is much clearer than in the original image.

Multistage ANN for Microcalcification Detection

After adaptive image enhancement, we extract features in order to find micro-calcification. Further on, multistage artificial neural network (ANN) is employed to detect the pixels that may belong to microcalcifications [4]. These features are obtained

using statistical characteristics of the gray level. The 1st stage ANN detects potential pixels which might be included in microcalcification. In the 1st stage ANN, every pixel in the breast area is used. Therefore, it takes much time to develop a high resolution mammogram image. To reduce this time consuming process, the size of the input image for the 1st stage of the ANN image is reduced to 1/4 of the original. These pixels are then grouped into one object with potential neighborhood pixels.

Input for the 2nd stage ANN is the one object which is detected by the 1st stage ANN with original image size. Detected objects in the 2nd stage ANN suggest a high probability of microcalcification. If more than 3 such objects are detected in a small area (radius < 80 pixel), the area is classified as a micro-calcification.

Fig. 3 shows an example of microcalcification detection results, where Fig. 3 (b) is an enhanced image with malignant microcalcification. The display in Fig. 3 (c) means that potential pixels and the pixels used as original content are one object. Fig. 3 (d) is a microcalcification detection result.
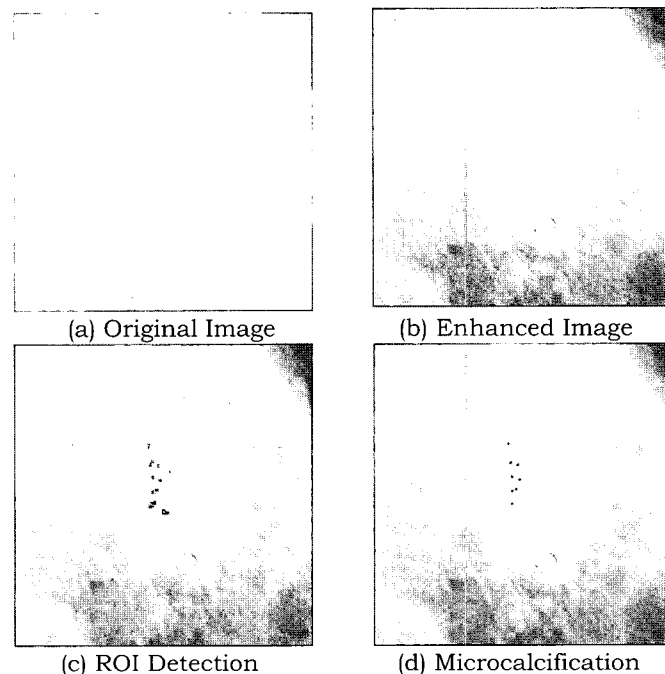

(a) Original Image   (b) Enhanced Image

(c) ROI Detection   (d) Microcalcification

Fig. 3. Example of microcalcification detection

To validate the proposed system, experiments were performed with a Digital Database for Screening Mammography (DDSM) database. In DDSM database, the resolution of a mammogram is 50 μm/pixel and gray level depths are 12 bits and 16 bits with various kinds of noise characteristics. The ANN training data and test data are obtained from the DDSM database.

The training database contains 56 cases of microcalcification and 56 cases of normal mammograms. The test data set contains 118 cases of microcalcification and 118 cases of normal mammograms.

To evaluate the performance of microcalcification detection, we measured TP (true positive) and FP (false positive) using two different enhancement methods. One is our proposed method and the other is the histogram stretching method. TP ratio means true positive detection ratio, which shows how many microcalcifications are detected. And FP number/image means the number offalse positives. The result of the histogram stretching TP ratio is 79.3%, for 0.75 FP number/image. In our proposed system, the TP ratio is 84.6% for 0.7 FP number/image. In experiments, our proposed system shows better results for every FP value.

DEVELOPMENT OF DIGITAL RADIOLOGICAL IMAGING TECHNIQUES

Digital radiological imaging has become an increasingly important part of the study of biological behavior of small animals and humans, allowing measurements of physiology, chemistry, and metabolic activity *in vivo*.

We are developing digital radiological imaging technology specifically designed for in-vivo molecular imaging. The aims of this work are to develop a simulation method for radiology instrumentation, a gamma-ray detector module using semiconductors, and a multi-modality imaging system. In order to achieve these goals, we have designed and simulated such processes from detectors to complete imaging systems; we have constructed detectors and complete prototype systems; and, we have developed a multi-modality imaging system.

Simulation Method for Radiology Instrumentation

Recently enhanced by the wider availability of powerful computer clusters, Monte Carlo simulations have become an essential tool for current and future radiology instrumentation development. Examples of research areas benefiting from these developments are the design of new medical imaging devices, the optimization of acquisition protocols, and the development and assessment of image reconstruction algorithms and correction techniques.

Currently, there are numerous Monte Carlo simulation packages for either positron emission tomography (PET) or single photon emission computer tomography (SPECT), each with different advantages, disadvantages and levels of reliability [6]. Accurate and versatile general-purpose

simulation packages such as Geant3, EGS4, MCNP and most recently Geant4 are available. These packages include well-validated physics models, geometry modeling tools and efficient visualization utilities. However, it is quite difficult to tailor these packages to PET and SPECT. In addition, the dedicated Monte Carlo codes developed for PET and SPECT suffer from a variety of drawbacks and limitations in terms of validation, accuracy and support.

Clearly, a Monte Carlo code is needed that is capable of accommodating complex scanner geometry and imaging configurations in a user-friendly way, while retaining the comprehensive physics modeling abilities of the general purpose codes. Furthermore, the need is to have a platform that can model decay kinetics, deadtime and movement, while benefiting from the same versatility and support as that of the general-purpose simulation codes. Object-oriented technology appeared to us to be the best choice to ensure high modularity and re-usability for PET and SPECT simulation tools. Therefore, we selected the simulation toolkit developed in C++ by the Geant4 collaboration, and decided to foster long-term support and maintenance by sharing code development among the many research groups that form the OpenGATE collaboration.

GATE, the Geant4 Application for Tomographic Emission [7], incorporates the Geant4 libraries in a modular, versatile and scripted simulation toolkit that is specifically adapted to the field of nuclear medicine. A public release of GATE licensed under the GNU Lesser General Public License (LGPL 1999) can be downloaded at http://www-lphe.epfl.ch/GATE/.

GATE was designed with several objectives in mind. First, the use of the GATE software should not require any knowledge of C++. End-users from the nuclear medicine community should be able to use GATE without worrying about the programming details. Second, since many nuclear medicine diagnostic techniques share similar concepts, GATE software components should be general enough to be reused from one context to another. Last, GATE should be modular, and thus be able to evolve as new applications are envisioned and develope
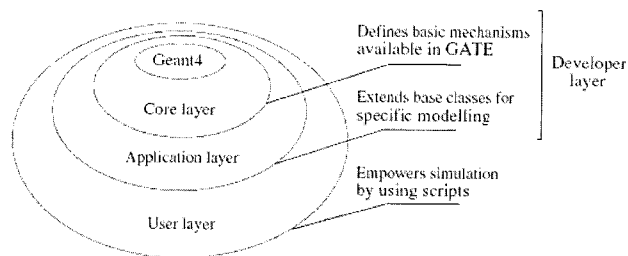

Fig. 4. Sketch of the layered architecture of GATE

The requirements discussed above are met using a layered architecture sketched in Fig. 4. The core of GATE, developed in C++, defines the main tools and features of GATE. The application layer is an extensible set of C++ classes based on the GATE core. On top of the application layer is the user layer, where end-users can simulate experiments using an extended version of the Geant4 scripting language. The complete set-up of scanner geometry and collimator can be easily defined using the script language, as shown in Fig. 5.
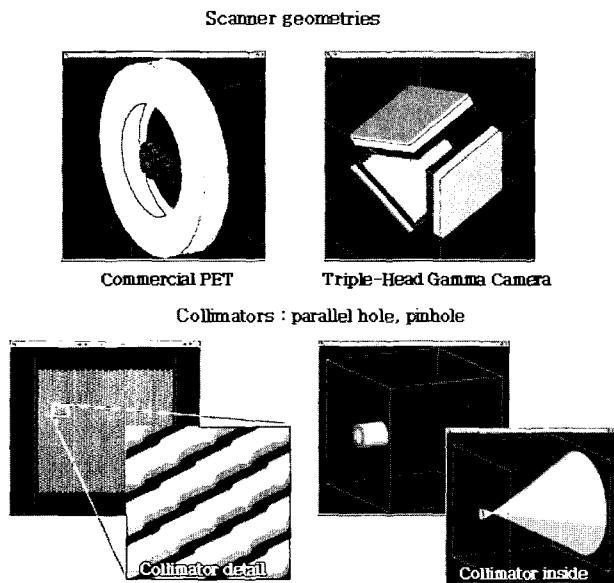
Scanner geometries

Commercial PET   Triple-Head Gamma Camera

Collimators : parallel hole, pinhole

Fig. 5. Example of scanner geometries and collimators simulated with GATE

Gamma-Ray Detector Module Using Semiconductor

The avalanche photodiode (APD) arrays represent a promising alternative to multi-anode or position-sensitive photomultiplier tubes (PMTs) for small animal PET [8]. Advantages of APD arrays over PMTs include the higher packing fraction and quantum efficiencies, the faster response, and the relative insensitivity to magnetic fields. During the last decade, the gain of APDs was markedly increased by implementing deep diffusion p-n junction structures, and this higher gain has come with improvements in detector noise performance. We have characterized the recently developed high gain APD arrays to evaluate their performance for PET.

Two new prototypes (Fig. 6) of APD arrays developed by Radiation Monitoring Devices (RMD) were

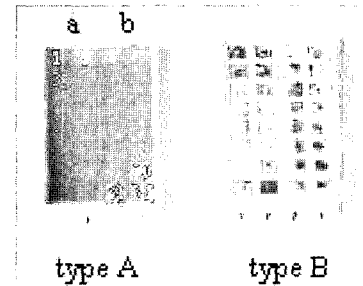investigated and compared with the A1604 array manufactured by RMD.

type A   type B

Fig. 6. Front view of the array A (left) and B (right)

They consist of two monolithic matrices having 2 × 8 beveled-edge-type deep diffusion pixel elements with an approximately 2×2 mm^2 sensitive area. Array A and B have different optical coatings. On array A, the anti-reflective coating appears somewhat uniformly mottled across the surface, whereas it appears smooth and multi-coloured on array B.

The relationship between capacitance and reverse bias voltage was measured using a digital capacitance bridge. For the gain measurements, a pencil beam with 450 nm wavelength was illuminated at the center of each pixel. At any given bias voltage, the gain value was determined by the ratio of that photocurrent to the photocurrent measured at 500 V, where the gain was assumed to be equal to 1. Since the APD gain and dark current were strongly dependent on temperature, two Peltier elements were used to control the APD substrate temperature, with an accuracy of 0.1°C. The bulk and surface contributions to the dark current of the APD were determined by linear fitting. Quantum efficiency and dark current measurements were compared with the APD array model A1604 from RMD.

Fig. 7 demonstrates the quantum efficiency versus wavelength for the different APD arrays. Table 1 gives the quantum efficiencies of arrays A, B, and A1604. Due to the addition of an optical coating, the quantum efficiencies of arrays A and B were markedly larger than those for array A1604. The mean quantum efficiency of type B was higher than that for type A, but the uniformity of the quantum efficiency for type A was better than that for type B. Fig. 8 shows the average dark currents over all pixels of a matrix measured as a function of gain at 22 °C. Surface and bulk leakage currents obtained from a linear fit were (24.7 ± 3.6) nA and (0.07 ± 0.02) nA for array A, (16.3 ± 3.6) nA and (0.07 ± 0.01) nA for array B.
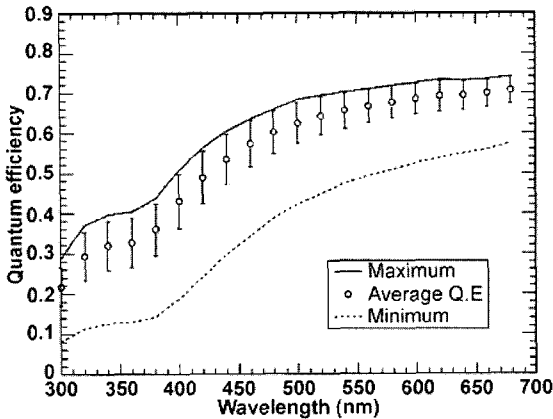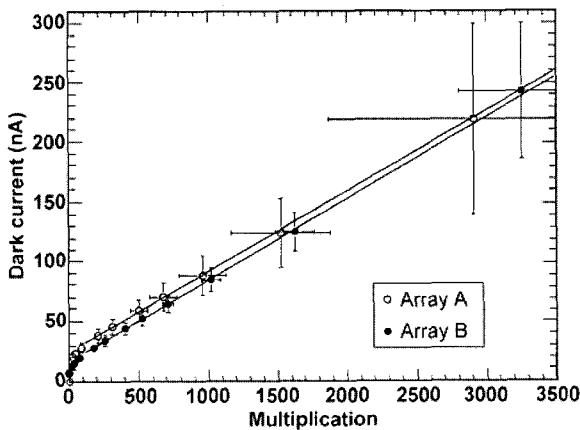
Fig. 7. Quantum efficiency versus

Fig. 8. Average dark currents with wavelength standard deviation versus gain

Table 1. Maximum, minimum, and mean quantum efficiency of array A, B, and A1604 at two wavelengths

Array	Type A		Type B		A1604	
λ [nm]	400	450	400	450	400	450
QE_{min}	0.38	0.52	0.37	0.50	0.36	0.45
QE_{max}	0.46	0.58	0.61	0.75	0.44	0.54
$<QE>$	0.41	0.54	0.50	0.65	0.39	0.49

Multi-Modality Imaging System

Functional images such as gamma-ray images can occasionally be difficult to interpret due to a lack of identifiable anatomical features. By combining images from an anatomical modality, such as X-ray CT, we can enhance our

understanding of the image and obtain complementary information about the object that can assist in the corresponding uptake of the radiotracer.

The combination of tomographic imaging modalities has been demonstrated to be useful in small animal imaging. Several groups have recently reported on their progress in the development of the fused imaging systems [9]. The aim of this study was to develop a compact SPECT/CT system for small animal imaging.

The SPECT system consisted of a pinhole collimator and a plate type scintillation crystal coupled to Hamamatsu (Shizuoka, Japan) R3292 PSPMT [10-12]. The scintillation crystal was NaI(Tl) plate measuring 6 mm in thickness and 120 mm in diameter. The focal length of the pinhole collimator was 45 mm and the acceptance angle was 90°. The SPECT system was mounted perpendicular to the X-ray system (Fig. 9).

The X-ray system consists of a microfocus X-ray source and a CMOS flat-panel detector [13]. The X-ray tube (UltraBright, Oxford Instruments) is a 80 W tungsten anode tube with maximum voltage of 90 kV and emits a cone-beam of X-rays. The CMOS flat-panel detector (C7943, Hamamatsu) consisted of a 1248 × 1248 active matrix-addressed array with CMOS thin-film transistors (TFTs), photodiode sensors having a pixel pitch of 100 μ m, and a CsI(Tl) scintillator.
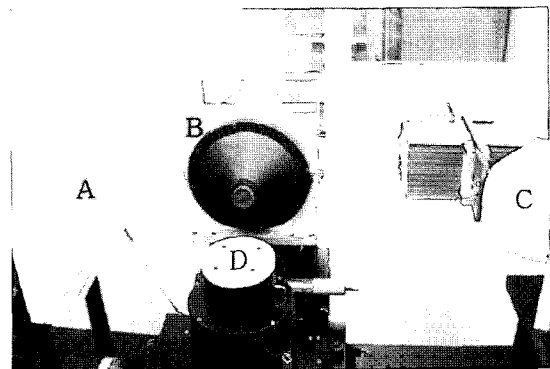

Fig. 9. Dual-modality system with A) a CMOS flat-panel detector, B) a pinhole SPECT detector, C) a microfocus X-ray source, and D) a motor. All the components of the dual-modality system except the data processing system were mounted on an optical table

DEVELOPMENT OF MEDICAL UNIFIED SOLUTION USING 3D IMAGE FUSION

The objective of this subproject is to develop a medical unified solution using 3D image fusion for the early diagnosis of musculoskeletal disease and

for the evaluation of the treatment of patients, including those with gait disorders, spinal disorder, etc. The detailed objectives are as follows:
- development of a solution for the diagnosis of these disorders and an evaluation of rehabilitation procedures;
- development of a solution for the improvement of sports performance ability; and,
- development of a solution for the prediction and evaluation of progress before and after surgery for spinal disorders.

Solution for Diagnosis of Disorders and Evaluation of Rehabilitation Procedures

A motion analysis approach using 3D imaging provides quantitative documentation of the subject's performance with reliable instrumentation that provides a permanent record of fact [14]. Therefore, this kind of approach has been regarded as a useful method in the biomechanical analysis of gait disorders using 3D image.

Gait disorder is any functional deformity that occurs when damaged tissues do not allow patients to maintain normal posture and range of motion during walking. Joint contractures are among the most common causes [15]. Equinus gait, which represents about 50% of pathological gaits, is the primary example of joint contracture [16]. However, there are no biomechanical severity indices, and only a few diagnostic systems exist to diagnose equinus gait and evaluate the rehabilitation process.

The Stanford Gait program was developed at the Stanford University as the first expert gait analysis system. This was followed by the GAITSPERT system at Vanderbilt University in the early 1980s. Recently, Dr.GaitⅢ has been introduced by the University of Texas at Houston in 1999. However, these expert gait systems are based on joint motion and electromyography (EMG) data which include skin artifact errors. Moreover, these are not able to provide analysis of muscle-tendon complex (MTC) motion and do not offer any specific treatment planning.

We have developed the Severity Index of Equinus Gait (SIEG) as a proposed solution. A three-dimensional (3D) heel contact pattern is used to calculate this severity index. 3D rear-foot motion can be normalized according to the foot length of each subject. The normalized rear-foot motion is integrated during the stance phase of a gait cycle (100%) so that the integrated value (SIEG) is presented as the severity of the equinus gait. We have also constructed the 3D MTC model which can evaluate the dynamic analysis of the muscle-tendon complex during walking. Fig. 10 and 11 illustrate SIEG and the anatomical schema for the 3D MTC model, respectively.
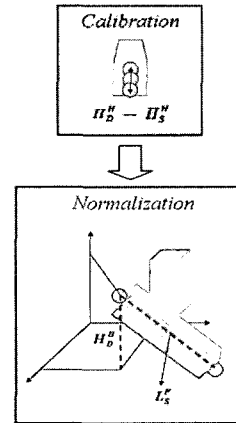

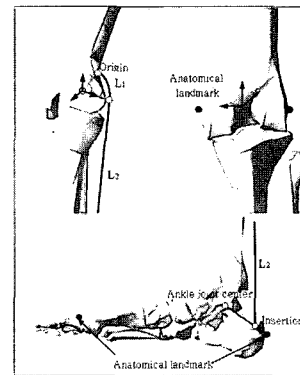
Fig. 10. SIEG (Severity Index of Equinus Gait)

Fig. 11. Anatomical schema for the 3D MTC Model

● Calibration using heel marker height :

$$H_D^H - H_S^H$$

H_D^H : Rear-foot marker position in the dynamic state

H_S^H : Rear-foot marker position in the static state

● Normalization using each subject's foot length:

$$(H_D^H - H_S^H)/L_S^F$$

H_D^H : Rear-foot marker position in the dynamic state

H_S^H : Rear-foot marker position in the static state

L_S^F : Length from heel to second metatarsal joint

● Parameters in muscle-tendon complex model
L1 = Radius of femoral condyle
L2 = Gastrocnemius-Achilles tendon complex length

Solution for the Improvement of Sports Performance Ability

A physically active lifestyle is important for all age groups. There are many reasons to participate in sports and physical activity, such as pleasure and relaxation, competition, maintenance, improvement of fitness and health. Golf is the one of the most popular sports in the world for people of all ages and skill levels. In fact, it appeals to people of almost all backgrounds with no regard for age, sex, socioeconomic status or level of physical fitness. Since power, accuracy and consistency are crucial requirements during a game of golf, several things have been tried to improve these factors.

In previous studies, some solutions for improving the golf swing (such as a golf clinic) have analyzed two-dimensional motion to better understand the characteristics of the golf swing [17,18]. The obvious appeal of such two-dimensional analysis is that it reduces both data collection and analytical time, as well as mathematical complexity [19]. However, a three-dimensional analysis of the golf swing is required because a meaningful interpretation of such kinetic data would better help both the instructor and the player to improve performance [19]. reaction patterns.

The special characteristics of the developed solution are as follows:

1) 3D kinetic and kinematic analysis;
2) Visualization using rendering technique; and,
3) Prediction of injuries related to golf activities.

Fig. 12 and 13 show the flowchart for the improvement of sports performance ability and the equipment used for motor analysis, respectively.
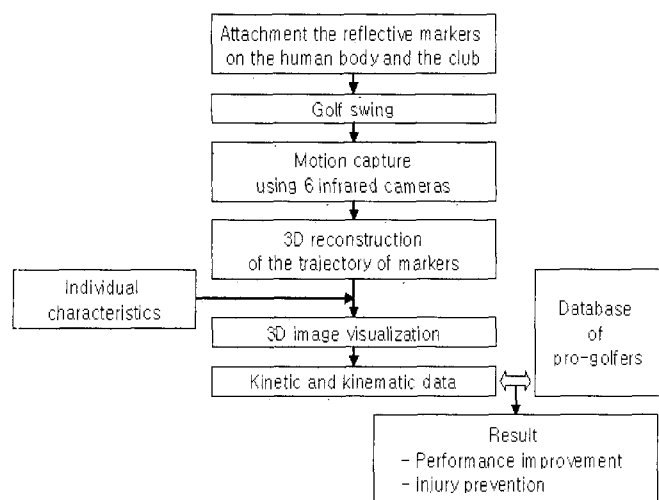

Fig. 12. The flowchart of solution for improvement of sports performance ability
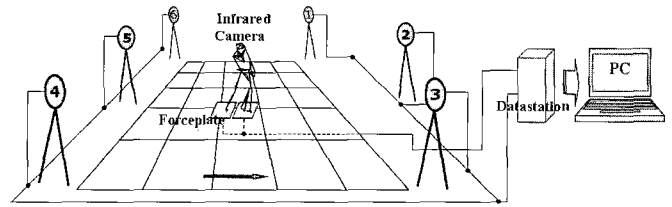

Fig. 13. Experiment setup

Table 2. Equipments for motion analysis

Equipment	Description
Infrared camera	The infrared camera converts the reflective light of marker into a video signal.
Forceplate	The forceplate analyzes weight transfer by measuring reaction forces
Datastation	The datastation is the hardware component which controls cameras and captures data.

Solution for Prediction and Evaluation of Progress Before and After Surgery

Injuries to the spine and spinal cord are common. Spine injuries include fractures and dislocations. These may or may not be associated with spinal cord injuries. Spinal cord injuries may be seen without spine injuries. Their causes include falls, motor vehicle accidents, blunt trauma, gunshot wounds, stab wounds and sports injuries. Spinal cord injuries are a significant cause of disability in young people. The majority of injuries are seen in the cervical (neck) spine followed by the thoracic (chest) spine and the lumbar (low back) spine.

We have developed a simulation spine model using a Finite Element (FE) method. The advantage of this model lies in its ability to predict both kinematic and internal stress profiles as a function of geometric and material property changes. For this reason, the FE method is ideally suited for the investigation of progressive disease states in which temporal degradation of certain structures alters their material properties.

In this study, the main aim of the developed model is to predict and evaluate progress of a patient before and after surgery. In the case of the cervical spine, the occipito- atlanto-axial joints maintains their stability mainly by using surrounding soft tissues, like other spines.

The transverse ligament of the atlas, by limiting anterior displacement of the atlas, is the strongest one among those. It protects the spinal cord. Several surgical methods have been tried for improving atlanto-axial stability and posterior fixation using wires has been widely used because of sufficient stability and a high rate of bony adhesion [21]. Generally, manipulation is difficult and the risk of neural injury is increased if the wire is thick. On the other hand, if the wire is too thin, the handling is relatively easy but resultant fixations are insufficient. Thus, a critical point for a surgeon in this case is how to decide upon the thinnest wire with a sufficient fixing force. We have simulated posterior fixation surgery [22] with diverse wires using an FE model for this purpose and predicted its results (Fig. 14).
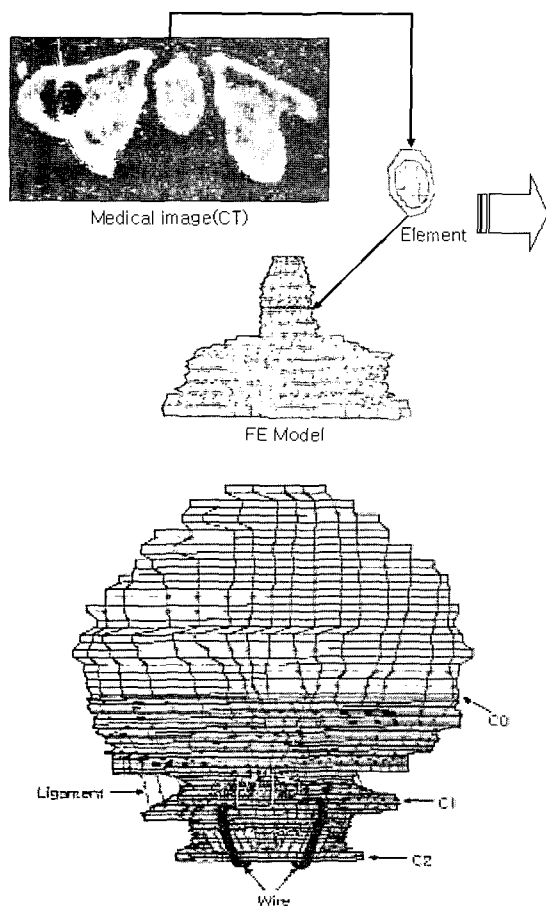

Fig. 14. Process of FE modeling and entire model for prediction of surgery

For other spinal problems, there have been many surgical methods used, such as posterior thoracic instrumentation and fusion for spinal deformity,

anterior thoracotomy discectomy with vertebrectomy and reconstruction, posterior lumbar inter-body fusion and instrumentation, the anterior lumbar retroperitoneal approach for lumbar fusion, anterior transperitoneal approach to the lumbar spine for fusion, and so on. It is necessary to evaluate quantitatively after such surgery if the progress of patient is satisfactory or not. Scoliosis, kyphosis and lordosis are general pathologies of the spinal curvature and all spinal deformities are due to some combination of these pathologies [23]. The analysis of spine segmental curvature change in a dynamic situation is critical for an understanding of spine pathological mechanisms [24]. Lumbar spine injury has been documented most frequently. It is estimated that 60-80% of the adult population has experienced low back pain. Thus, the lumbar spine should be analyzed in a dynamic perspective, including kinetic analysis [25, 26]. In other words, one needs to measure shear forces because poor segmental control of the lumbar spine can lead to increased shear force on the vertebral segments, causing breakdown and subsequent pathology. Thus, we plan to divide the spine using a linked segment model divided into six parts (C7/T1, T6/T7, T12/L1, L3/L4, L5/S1) [26] and to evaluate the progress of the patient at the joint before and after spine surgery based on kinematic and kinetic results.

DEVELOPMENT OF MULTI-PURPOSE DIGITAL ENDOSCOPY

The digital endoscopy system in general use obtains image signals from the distal tip of a CCD by illuminating the interior of a body through a light bundle emanating from an intrinsic light source system [27]. It incorporates a light source for providing images and a filtering system for transmitting the color images captured. Since induced color image signals are transmitted to a display device through the image center in the digital endoscopy system, they are helpful to diagnose whether biopsy is. As a result, misdiagnosis and unnecessary biopsy can be avoided [28].

The purpose of this study is to develop multi-purpose digital endoscopy using a Near Infra-Red (NIR) filter wheel system and to develop a hardware and software system. Hardware development consists of an imaging system, system controller and multi-filter wheel automation system using one microprocessor.

Software development for analysis of endoscopic images consists of pattern recognition algorithms, a disease region detection algorithm using discriminant analysis and back propagation network, and an image tracking algorithm using 3D information from the endoscopic image.

Filter Wheel System Development

The filter wheel, which is generally found with digital endoscopes, was connected to the light source system for high quality color images in an endoscope using CCD. The filter wheel system was developed for effectively detecting abnormal areas in the digital image using the NIR band-pass filter. Fig. 15 shows the structure of a general endoscope and image-obtaining procedures [29].

This system was connected to a common light source system and a threaded RC servo motor for correct angle adjustment. In addition, power transmission was composed of a timing-belt and timing-pulley to reduce position error caused by the motor. The controller system used a one-chip microprocessor to synchronize the NIR filters in the filter wheel with the light source system (Fig. 16).
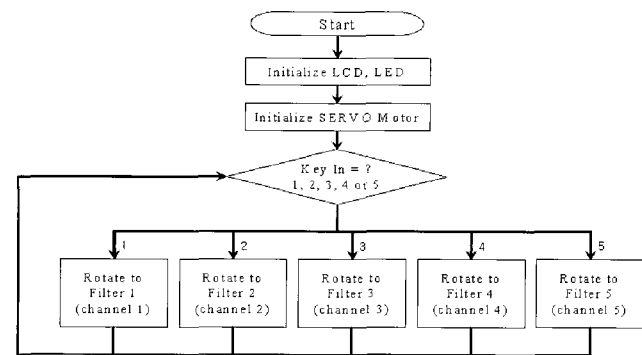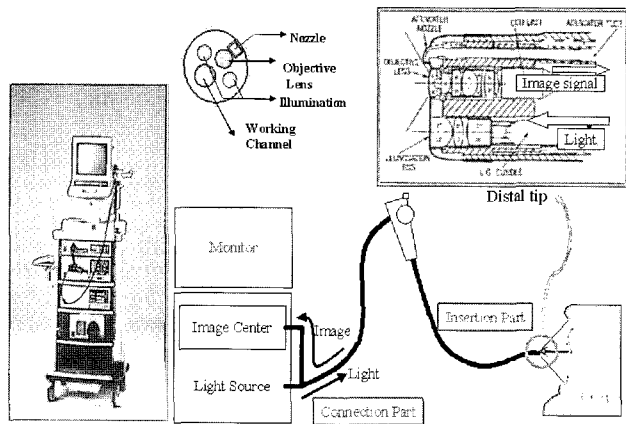
NIR (Near Infra-Red) Spectrum Analysis

Near InfraRed Spectroscopy (NIRS) was used for the first time in agriculture by Karl Norris in the 1960s. Near infrared is used primarily in component analysis of samples and mid infrared is used in functional group analysis. NIRS is used in the chemical component analysis of a sample [30].

NIR wavelength band width was used to measure chemical components in nude mice and to develop the NIR filter wheel system by using the infrared spectrometer (1100 ~ 1700 nm) and test equipment, which was designed and built for this research (Fig. 17, 18).
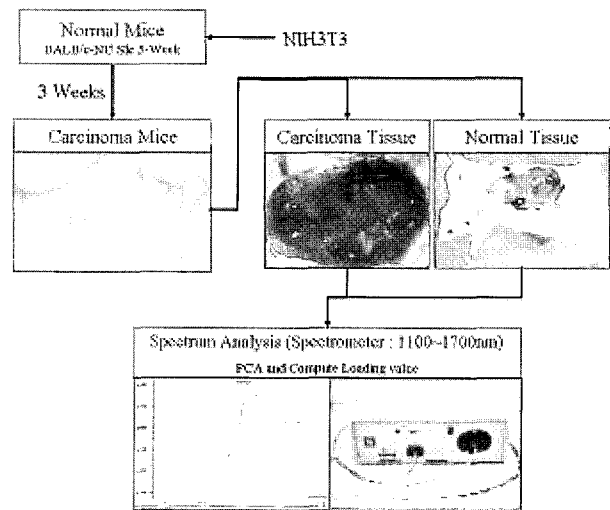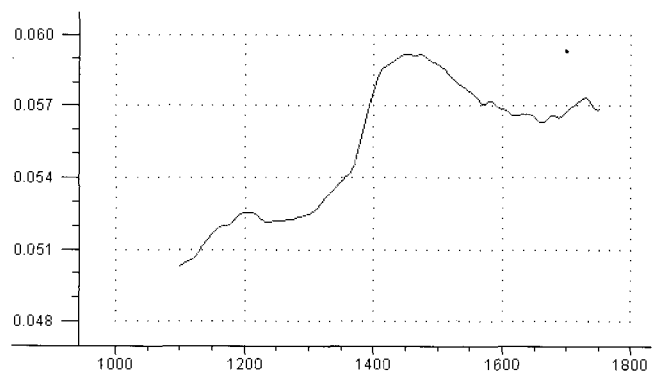

Fig. 17. The flowchart of spectrum analysis

Fig. 16. Flow Chart of Control Programming

Fig. 18. Loading for Cancer and Normal tissue using Spectrometer(1100~1700 nm)

Table 3. Image parameters

Color Parameters		Texture Parameters		
R Value	Hue Value	Maximum Probability	Entropy	K3
G Value	L value	Moment	Energy	K4
B Value	a Value	Homogeneity	Correlation	K5
Gray Value	b Value	Contrast	K	K6

Detection Algorithm

This study was carried out to develop detection algorithms for abnormal tissues in the body using image processing. Detection algorithms were developed to provide information from the digital images in order for a doctor to more correctly diagnose inflammation and ulceration.

This research was developed using an image segment algorithm to distinguish between normal and abnormal parts of endoscopic images by applying both color and texture parameters to the discriminant analysis and the Back Propagation Network (BPN) (Fig. 19). Table 3 shows image parameters [31, 32].

As the result of the discriminant analysis, the rate of success is indicated as 92.8% at the stage of compensation and as 92.4% at the stage of verification. In addition, through the BPN, the rate of success was 97.9% at the stage of compensation and 96.8% at the stage of verification. Therefore, the BPN proved to be more effective than discriminant analysis using statistical methods. Furthermore, the success rate of distinguishing normal from abnormal parts was utilized to find the number of neurons on the hidden layer of an artificial neural network. Learning parameters, which could distinguish between normal and abnormal parts, were obtained.
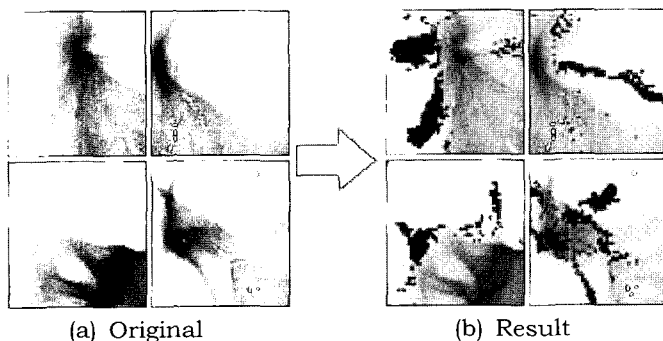
(a) Original   (b) Result

Fig. 19. Original and result images

APPLICATIONS AND FUTURE PLANS

The incidence of women's breast cancer is high, and breast cancer has a high mortality rate. Early cancer detection can reduce this mortality. Generally, the detection of microcalcification and mass is a major part of the diagnosis in the early stages of breast cancer. In this project, we propose a microcalcification detection CAD system for digital mammography, which automatically indicates suspicious areas of breast tissue.

GATE was publicly released in 2004. It makes it possible to model any real or proposed SPECT and PET scanners, and to realistically provide static or dynamic activity distributions in humans or small animals. The accuracy of GATE modeling has been extensively validated for various commercial SPECT and PET scanners and for prototypes. GATE can be used for optimizing scanner design and imaging protocols. Current developments with GATE include the implementation of acceleration techniques to speed up the simulations, incorporation of features to ease the use of GATE for dosimetric purpose, and user-friendly deployment of GATE on clusters and grids.

The main characteristics of two deep-diffusion APD array prototypes designed by RMD were investigated and compared to the RMD A1604 model. Due to the addition of an optical coating, these arrays have a higher quantum efficiency than the A1604 array. The anti-reflective coating is promising, but the method used to deposit it needs to be improved to ensure uniform and optimal thickness. An evaluation of the performance of the prototypes used as a photodetector coupled with a scintillator to detect 511 keV gamma rays is being performed.

The full potential of functional imaging can be realized only when areas of tracer uptake can be unambiguously assigned to organs or other anatomical features. Since well chosen radiotracers may have excellent uptake in the target, for example a tumor, but rapidly clear from surrounding tissues, functional images sometimes contain few recognizable anatomical features. The addition of independently measured and co-registered

anatomical information overcomes this limitation. The fused SPECT/CT system developed in this study provides high-quality images from both modalities and could be useful in obtaining functional images with high resolution morphologic information.

Motion analysis using images will help not only surgeons to determine the severity of equinus gait conditions and be able to offer the appropriate treatment to patients, but also helpful for people who want to improve their sports performance.

Our developed FE model can be used to identify specific structure involvement in the development and progression of disorder such as rheumatoid arthritis (RA), to identify localized osseous stresses due to global loading conditions, to evaluate the mechanical effectiveness of a new fixation system, and related items.

Diagnosis using endoscopic image processing does not require much time, and endoscopic imaging can easily detect diseases. In addition, the excellent resolution of an endoscope image allows greater accuracy for therapy, as well as for diagnosis [33]. Using a light source of the near infrared region with a specific wavelength band, this system can distinguish abnormal from normal tissue according to chemical components and characteristics, and thus can be helpful in recognizing diseases. Furthermore, this system might greatly contribute to the development of robots for surgical operations using the endoscope.

REFERENCES

[1] T.C. Wang and N.B. Karayiannis, "Detection of Microcalcifications in Digital Mammograms Using Wavelets", IEEE Trans. Med. Imag., Vol. 17, No. 4, pp. 498-509, 1998.

[2] A. Laine, J. Fan, and W. Yang, "Wavelets for Contrast Enhancement of Digital Mammography", IEEE Eng. in Med. and Bio. Mag., Vol. 145. pp. 536-550, 1995.

[3] H.K. Kang, S.M. Kim, N.N. Thanh, and Y.M. Ro, "Robust Contrast Enhancement for Microcalcification in Mammography", LNCS, Vol. 3045, pp. 602-610, 2004.

[4] H.K. Kang, S.M. Kim, N.N. Thanh, Y.M. Ro, and W.H. Kim, "Adaptive Microcalcification Detection in Computer Aided Diagnosis", LNCS, Vol 3039, pp.1110-1117, 2004.

[5] J.H. Yoon and Y.M. Ro, "Enhancement of the Contrast in Mammographic Images Using the Homomorphic Filter Method", IEICE Trans. Inform. and Sys., Vol.85-D, No.1, pp.291-297, 2002.

[6] I. Buvat and I. Castiglioni, "Monte Carlo simulations in SPECT and PET", Q. J. Nucl. Med., Vol. 46, pp.48-61, 2002.

[7] G. Santin, D. Strul, D. Lazaro, L. Simon, M. Krieguer, M.M. Vieira, V. Breton and C. Morel, "GATE: A Geant4-based simulation platform for PET and SPECT integrating movement and time management", IEEE Trans. Nucl. Sci., Vol. 50, pp.1516-1521, 2003.

[8] B. Pichler, G. Boening, E. Lorenz, R. Mirzoyan, W. Pimpl, M. Schwaiger, and S.I. Ziegler, "Studies with a prototype high resolution PET scanner based on LSO-APD modules", IEEE Trans. Nucl. Sci., Vol. 45, pp.1298-1302, 1998.

[9] G.A. Kastis, L.R. Furenlid, D.W. Wilson, T.E. Peterson, H.B. Barber, and H. H. Barrett, "Compact CT/SPECT Small-Animal Imaging System", IEEE Trans. Nucl. Sci., Vol. 51, pp.63-67, 2004

[10] J.H. Kim, Y. Choi, K.S. Joo, B.S. Sihn, J.W. Chong, S.E. Kim, K.H. Lee, Y.S. Choe and B.T. Kim, "Development of a miniature scintillation camera using NaI(Tl) scintillator and PSPMT for scintimammography", Phys. Med. Biol., Vol. 45, No.11, pp.3481-3488, 2000

[11] T.Y. Song, Y. Choi, Y.H. Chung, J.H. Jung, Y.S. Choe, K.H. Lee, S.E. Kim, and B.T. Kim, "Optimization of pinhole collimator for small animal SPECT using Mote Carlo simulation", IEEE Trans. Nucl. Scien, Vol. 50(3), pp.327-332, 2003

[12] T.Y. Song, Y. Choi, J.H. Jung, B.J. Min, K.J. Hong, Y.S. Choe, K.H. Lee, and B.T. Kim, "Performance Amelioration for Small Animal SPECT Using Optimized Pinhole Collimator and Image Correction Technique", Conf. Rec. of the 2004 IEEE NSS and MIC, Rome, Italy, 2004.

[13] S.C. Lee, H.K. Kim, I.K. Chun, M.H. Cho, S.Y. Lee, and M.H. Cho, "A flat-panel detector based micro-CT system: performance evaluation for small-animal imaging", Phys. Med. Biol., Vol. 48, pp.4173-4185, 2003.

[14] P. Jacquelin, Gait analysis: normal and pathological function, Chief of Patholokineology Rancho Los Amigos Medical Center Downey, CA, 1992.

[15] P.S. Edwards, Toe walking: Article, E_medicine, 2004.

[16] S.O. Michael, D.A. Michael, D.D. Robin, A.P. Rosemary, "Length and force of the gastrocnemius and soleus during gait following tendo Achilles lengthenings in children with equinus", Gait and Posture 15, 130-135, 2002.

[17] N. Nagao, and Y. Sawada, "A kinematic analysis of the golf swing by means of fast motion picture in connection with wrist action", J. Sports Med., Vol. 17, pp.413-419, 1977.

[18] S. Carlsoo, "A kinetic analysis of the golf swing", J. Sports Med., Vol. 7, No. 2, pp.76-82, 1967.

[19] C.L. Vaughan, A three dimensional analysis of the forces and torques applied by a golfer during the downswing, Biomechanics VII-B, 325-331. Baltimore: University Park Press, 1981.

[20] R.A. Mann, and J. Hagy, "Biomechanics of walking, and sprinting", J. Sports Med. Vol. 8, pp.345-350, 1980.

[21] S.J. Mixter and R.B. Osgood, "Traumatic lesion of the atlas and axis", Ann of surgery, pp.51-193, 1910.

[22] A.L. Brooks and E.W. Jenkins, "Atlanto-axial arthrodesis by the wedge compression method", J. Bone. Joint. Surg., Vol. 60-A, pp.279-284, 1978.

[23] C. Frigo, R. Carabalona, M. Dalla Mura, and S. Negrini, "The upper body segmental movements during walking by young females", Clinical Biomechanics, Vol. 18, No. 5, pp.419-425, 2003.

[24] C. Jack, V. Roongtiwa, and S. Richard, "Patterns of spinal motion during walking", Gait & Posture, Vol. 5, No. 1, pp.6-12, 1997.

[25] P.C. Jack, E.P. Aftab, and M.M. Stuart, "Low back three-dimensional joint forces, kinematics, and kinetics during walking, Clinical Biomechanics", Vol. 14, No. 3, pp.203-216, 1999.

[26] W.W. Michael and L. David, "Three-dimensional relationships between the movements of the pelvis and lumbar spine during normal gait, Human Movement Science", Vol. 18, No. 5, pp.681-692, 1999.

[27] J. Dijkstra and G. Koning, "Automatic Border Detection In IntraVascular Ultrasound images for Quantitative Measurements of the Vessel, Lumen and Stent Parameters", Leiden University Medical Center,

Leiden the Netherlands, 2001.

[28] L.M. Gao and Y. Chen, *"Micro Motor Based A new type of endoscope"*, Proceedings of the 20th annual international conference of the IEEE engineering in medicine and biology society, Vol. 20, No. 4, 1998.

[29] A. Paolo and B. Adriano, *"Image processing for medical diagnosis using CNN"*, Nucl. Instrum. Meth. A., Vol. 497, pp.174-178, 2003.

[30] S.H. Lee and A. Noam, *"Automated Quantitation of Non-Steady Flow and Lumen Area Based on Temporal correlation"*, Proceedings of the 23rd Annual EMBS International Conference, 2001.

[31] T. Shinichi, H. Masatsugu, *"Intrabody Three-Dimensional Position Sensor for an Ultrasound Endoscope"*, IEEE Trans. Bio. Eng., Vol. 49 No. 10, 2002.

[32] S. Mavromatis and J.M. Boi, *"Medical Image Segmentation Using Texture Directional Features"*, Proceedings of the 23rd annual EMBS international conference 2001.

[33] O. Timo, P. Matti, *"Multiresolution Gray-Scale and Rotation Invariant Texture Classification with Local binary Patterns"*, IEEE Trans. Patt. Anal. Machine Intell., Vol. 24, No. 7, 2002.